Cancer Letters 466 (2019) 23–34

Contents lists available at ScienceDirect

Cancer Letters

journal homepage: www.elsevier.com/locate/canlet

Original Articles

Dual-targeting of EGFR and Neuropilin-1 attenuates resistance to EGFR-targeted antibody therapy in KRAS-mutant non-small cell lung cancer

Ye-Jin Kim[a], Du-San Baek[a], Seyoung Lee[a], Daechan Park[b], Han Na Kang[c], Byoung Chul Cho[d,**], Yong-Sung Kim[a,e,*]

[a] Department of Molecular Science and Technology, Ajou University, Suwon, Republic of Korea
[b] Department of Biological Sciences, Ajou University, Suwon, Republic of Korea
[c] JE-UK Institute for Cancer Research, JEUK Co. Ltd., Gumi, Kyung-Buk, Republic of Korea
[d] Division of Medical Oncology, Yonsei Cancer Center, Yonsei University College of Medicine, Seoul, Republic of Korea
[e] Department of Allergy and Clinical Immunology, Ajou University School of Medicine, Suwon, Republic of Korea

ARTICLE INFO

Keywords:
KRAS mutation
Integrin β3
Bispecific antibody
Cetuximab resistance
EGFR/NRP1 dual-targeting

ABSTRACT

The therapeutic targeting of oncogenic KRAS mutant-harboring (KRAS^{MUT}) non-small cell lung cancer (NSCLC) is an urgent unmet need in cancer therapy. Although NSCLC is often driven by epidermal growth factor receptor (EGFR) overexpression and/or mutations, no EGFR-targeted therapy is clinically available for KRAS^{MUT} NSCLC. In this study, we show that integrin β3 expression is associated with the intrinsic resistance of KRAS^{MUT} NSCLCs to the anti-EGFR antibody cetuximab. Further analyses identified an integrin β3-mediated ternary complex comprising NRP1–integrin β3–KRAS^{MUT} and its downstream signaling of PI3K-Akt and RalB-TBK1 as a primary resistance mechanism of KRAS^{MUT} NSCLC to cetuximab treatment. Importantly, we demonstrate that the EGFR/NRP1 dual-targeting bispecific antibody, Ctx-TPP11, attenuates the downstream signaling driven by the ternary complex via the cellular co-internalization and degradation of the NRP1-coupled complex, resulting in the alleviation of cetuximab resistance in KRAS^{MUT} NSCLCs *in vitro* and *in vivo*, including patient-derived xenograft mouse models. Our study shows that the dual-targeting of EGFR and NRP1 with a bispecific antibody might be an effective therapeutic strategy for KRAS^{MUT} NSCLC.

1. Introduction

Non-small-cell lung cancer (NSCLC) represents ~80–85% of all lung cancers and is associated with an overall 5-year survival rate of less than 15% [1]. Given that it is often driven by epidermal growth factor receptor (EGFR) overexpression and/or mutations [2], several EGFR tyrosine kinase inhibitors (EGFR-TKIs) (e.g., gefitinib, erlotinib, and afatinib) and one anti-EGFR antibody (Ab) necitumumab (Portrazza) have been approved in combination with chemotherapy for the treatment of advanced NSCLC [3,4].

Oncogenic activating *KRAS* mutations are found in approximately 20–30% of NSCLC patients [4,5], and these correlate with poor clinical prognosis [6] and have shown to be associated with primary resistance to EGFR-targeted therapy [7–9]. A recent study showed that the mutant KRAS (KRAS^{MUT}) protein physically interacts with integrin β3 to promote RalB-TBK1-mediating resistance to the EGFR-TKI erlotinib in KRAS^{MUT} NSCLC [10]. These findings highlight the need for a concomitant KRAS^{MUT}-targeting strategy based on the inhibition of EGFR for KRAS^{MUT} NSCLC. However, no drugs directly targeting KRAS^{MUT} are now clinically available [11–13] and clinical trials on small molecule inhibitors of KRAS^{MUT} downstream pathways (e.g., the MEK inhibitor selumetinib) have failed to improve the survival of patients with KRAS^{MUT} NSCLC [7,14]. Accordingly, new strategies to simultaneously target both EGFR and KRAS^{MUT} pathways are urgent to improve treatment for KRAS^{MUT} NSCLC.

Our group has previously reported that co-targeting EGFR and neuropilin-1 (NRP1) with the bispecific antibody (bsAb), Ctx-TPP11, overcomes the resistance of pancreatic ductal adenocarcinoma (PDAC) to anti-EGFR Ab cetuximab [15]. Ctx-TPP11 was generated by the genetic fusion of the NRP1-targeting peptide TPP11 to the C-terminus of the heavy chain of cetuximab [16]. Ctx-TPP11 was found to down-regulate active integrin β1 levels through NRP1-coupled internalization mediated by the TPP11 moiety, leading to the inhibition of active integrin β1-driven signaling, which facilitates cetuximab resistance, in

---

[*] Corresponding author. Department of Molecular Science and Technology, Ajou University, Suwon, Republic of Korea.
[**] Corresponding author.
E-mail addresses: cbc1971@yuhs.ac (B.C. Cho), kimys@ajou.ac.kr (Y.-S. Kim).

https://doi.org/10.1016/j.canlet.2019.09.005
Received 9 July 2019; Received in revised form 9 September 2019; Accepted 11 September 2019

PDACs [15]. NRP1, a non-tyrosine kinase receptor functioning as a co-receptor for other cell surface receptors such as integrins, is overexpressed in diverse solid tumors and plays a critical role in tumorigenesis, metastasis, and angiogenesis [17,18]. Further, its overexpression is associated with poor outcome in NSCLC patients [19,20].

In this study, we aimed to identify the mechanism(s) of resistance to the anti-EGFR Ab cetuximab in KRAS^{MUT} NSCLC and test a therapeutic strategy comprising EGFR/NRP1 dual-targeting with the Ctx-TPP11 bsAb to sensitize KRAS^{MUT} NSCLCs *in vitro* and *in vivo*, including patient-derived xenograft (PDX) models.

2. Materials and methods

2.1. Reagents and antibodies

LY294002 (440202) was purchased from Millipore. Sorafenib (S7397) and BX-795 (S1274), afatinib (S1011), erlotinib (S7786), pictilisib (S1065), buparlisib (S2247), trametinib (S2673), and RO5126766 (S7170) were purchased from Selleckchem. Hoechst 33342 (H3570) was from Invitrogen. Antibodies used as reagents in this study are listed in Supplementary Table S3.

2.2. Expression and purification of antibodies

Mammalian expression plasmids for Fc-TPP11, cetuximab, and Ctx-TPP11 were described previously [15,16]. Expression plasmids for anti-EGFR Abs (necitumumab, nimotuzumab, and matuzumab) and their IgG-TPP11 formats were constructed in the same manner as Ctx-TPP11. All constructs were confirmed by sequencing (Macrogen, Inc.). All antibodies were expressed by transient transfection into HEK293F cell cultures, purified, and dialyzed against a final buffer of Dulbecco's phosphate-buffered saline (PBS, pH 7.4), as described previously [11,15]. The details are described in the Supplementary Methods.

2.3. Cell lines

The human NSCLC cell lines, Calu-3, HCC827, HCC44, A549, SK-LU-1, Calu-6, H1299, HCC2108, H2009, H358, and H460 were purchased from the Korean Cell Line Bank (KCLB) and PC-9, H1975, H2030, and H441 cells were purchased from the American Type Culture Collection (ATCC). The authenticity of these cell lines was verified based on the genomic short tandem repeat profile of each cell line (ABION, Korea). All cell lines in this study except Calu-3 cells were cultured in RPMI1640 (HyClone; SH30027-01), supplemented with 10% fetal bovine serum (HyClone; SH30919-03) and 1% antibiotic–antimycotic solution (Welgene; LS 203-01). Calu-3 cells were cultured in Minimum Essential Media (MEM; HyClone; SH30024-01) with 10% fetal bovine serum and 1% antibiotic–antimycotic solution at 37 °C in 5% CO_2. Mycoplasma was often checked using the TransDetec LucifeRASe Mycoplasma Detection Kit (TransGen Biotech, Beijing).

2.4. Cell proliferation assay

Cells, seeded at a density of 5×10^3 cells/well in 96-well plates, were grown for 12 h, and then treated with agents and/or pharmacological inhibitors for 48 h as specified in the figure legends. After incubation for 48 h, cell proliferation was determined using a metabolic activity (dehydrogenase)-based EZ-CytoX cell viability assay kit (LPS Solution, Korea). The water-soluble tetrazolium salt (WST) reagent (10 μl/well) was added to each well, and absorbance was read at 450 nm after a 1- or 2-h incubation at 37 °C. The results are presented as a percentage of the value obtained from the drug vehicle-treated control group. The dose-dependent data was used to estimate IC_{50} value (the concentration causing 50% inhibition of cell proliferation) by fitting it to a non-linear sigmoidal curve using GraphPad Prism 5 software.

2.5. In vivo cell line-derived xenograft (CDX) treatment

All procedures were approved by the Animal and Ethics Committee of Ajou University Medical Center (approval ID No. 2017-0011) and performed in accordance with the guidelines established by the Institutional Animal Care and Use Committee. Calu-6 (1×10^7 cells per mouse) and H460 NSCLC cells (2×10^7 cells per mouse) in 150 μl of a 1:1 mixture of PBS/Matrigel (BD Biosciences, 354234) were injected subcutaneously into the right thigh of 4-week-old female BALB/c nude mice (Charles River Japan) weighing 17–20 g and were grown as tumor xenografts. When tumor volume reached approximately 200–300 mm^3, mice were randomly assigned to drug treatment groups ($n = 6$ per group) and treated with proteins or antibodies via the tail vein, in a dose/weight-matched manner, as specified in the figure legend. Tumor volume (V) was evaluated using calipers and estimated by formula $V = L \times W^2/2$, where L and W are the longest and shortest lengths of the tumor, respectively [11]; tumor volumes and body weight were recorded at regular intervals. Tumor growth inhibition (TGI) by Ctx-TPP11 compared to that with cetuximab was determined on the last day of the study according to the formula: $\mathrm{TGI}\ (\%) = (100 - (V_f^{\mathrm{Ctx-TPP11}} - V_i^{\mathrm{Ctx-TPP11}})/(V_f^{\mathrm{cetuximab}} - V_i^{\mathrm{cetuximab}}) \times 100)$, where V_i and V_f were the initial and final mean tumor volumes, respectively, in the Ctx-TPP11 or cetuximab treatment groups [11]. Mice were euthanized via CO_2 asphyxiation, and some tumors were collected for western blotting and immunohistofluorescence analysis as published [11,15].

2.6. In vivo PDX treatment

Tumor specimens from malignant effusions of patients with NSCLC were collected at Yonsei University Severance Hospital. The study protocol was approved by the institutional review board of Severance Hospital (4-2013-0526), and all patients gave written informed consent before sample collection. To establish PDX models, 5–7-week-old female severe combined immunodeficient (NOG) and nude (nu/nu) mice (OrientBio, Seoul, Korea) were used. Tumor tissue obtained from F1 mice were excised and cut into small ($3 \times 3 \times 3$ mm^3) fragments and then implanted subcutaneously into a group of five to six mice for each patient. When the tumors size reached ~1.5 cm in diameter, they were excised and dissected into fragments ($3 \times 3 \times 3$ mm^3) and implanted into another set of mice according to the same procedure. The passage harboring the patient-derived material was termed F0, with subsequent generations numbered consecutively (F1, F2, F3, and so on) [21]. The F3 generation was expanded for *in vivo* drug efficacy tests. The tumors and related PDXs were assigned Yonsei Human In Mouse (YHIM) identifiers that corresponded to the original patient-derived tumors. For *in vivo* antibody treatment studies, when tumors were established at volumes of 200–250 mm^3, mice were randomized into five treatment groups. Cetuximab and Ctx-TPP11 were administered intraperitoneally at 10 mg/kg every 3 days. Tumor dimensions were measured twice per week with digital calipers and tumor volume was calculated by the formula described previously herein. Tumor tissues were excised and analyzed by immunohistochemical analysis, as described [22].

2.7. Other methods

Since the following procedures have been performed according to the previously reported methods, they are described in detail in the Supplementary Methods along with any modifications to the procedures as follow: flow cytometry [15,16], RNA interference [15], Genomics of Drug Sensitivity in Cancer (GDSC) database analysis [23], immunoprecipitation (IP) and western blotting [11,15], confocal immunofluorescence microscopy [15], and immunohistochemical analysis of tumor tissues [11,15].

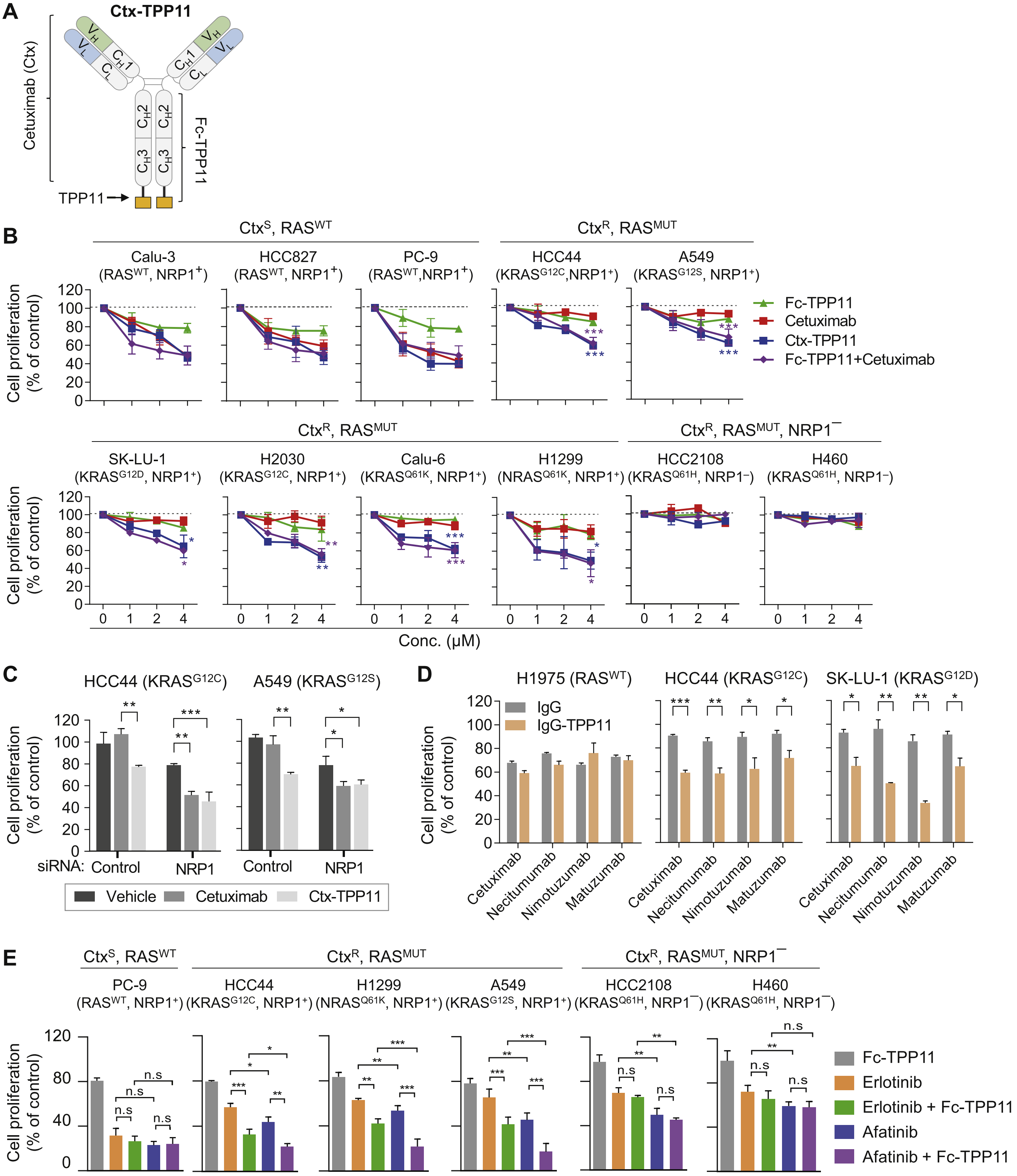

Fig. 1. Co-targeting of EGFR and NRP1 attenuates the resistance of $KRAS^{MUT}$ NSCLCs to anti-EGFR antibody treatment. (**A**) Schematic diagram of Ctx-TPP11 bsAb, in which the NRP1-targeting TPP11 peptide was genetically fused via a $(G_4S)_3$ linker to the C-terminus of the heavy chain of cetuximab. (**B**) Cell proliferation assay after cells were treated with agents at the indicated concentrations for 48 h. (**C**) Effect of NRP1 knockdown on the proliferation of cells treated with indicated agents (2 μM) for 48 h. (**D**) Cell proliferation assay after cells were treated with indicated agents (2 μM) for 48 h. (**E**) Cell proliferation assay after cells were treated for 48 h with the indicated agent (8 μM) with or without Fc-TPP11 (4 μM). In (B–E), error bars, ± SD (n = 3); $*P < 0.05$, $**P < 0.01$, $***P < 0.001$ versus cetuximab-treated cells (B) or between the indicated samples (C–E); n.s., not significant (E). In (B), statistical analysis was performed using a one-way analysis of variance followed by the Newman-Keuls post-hoc test.

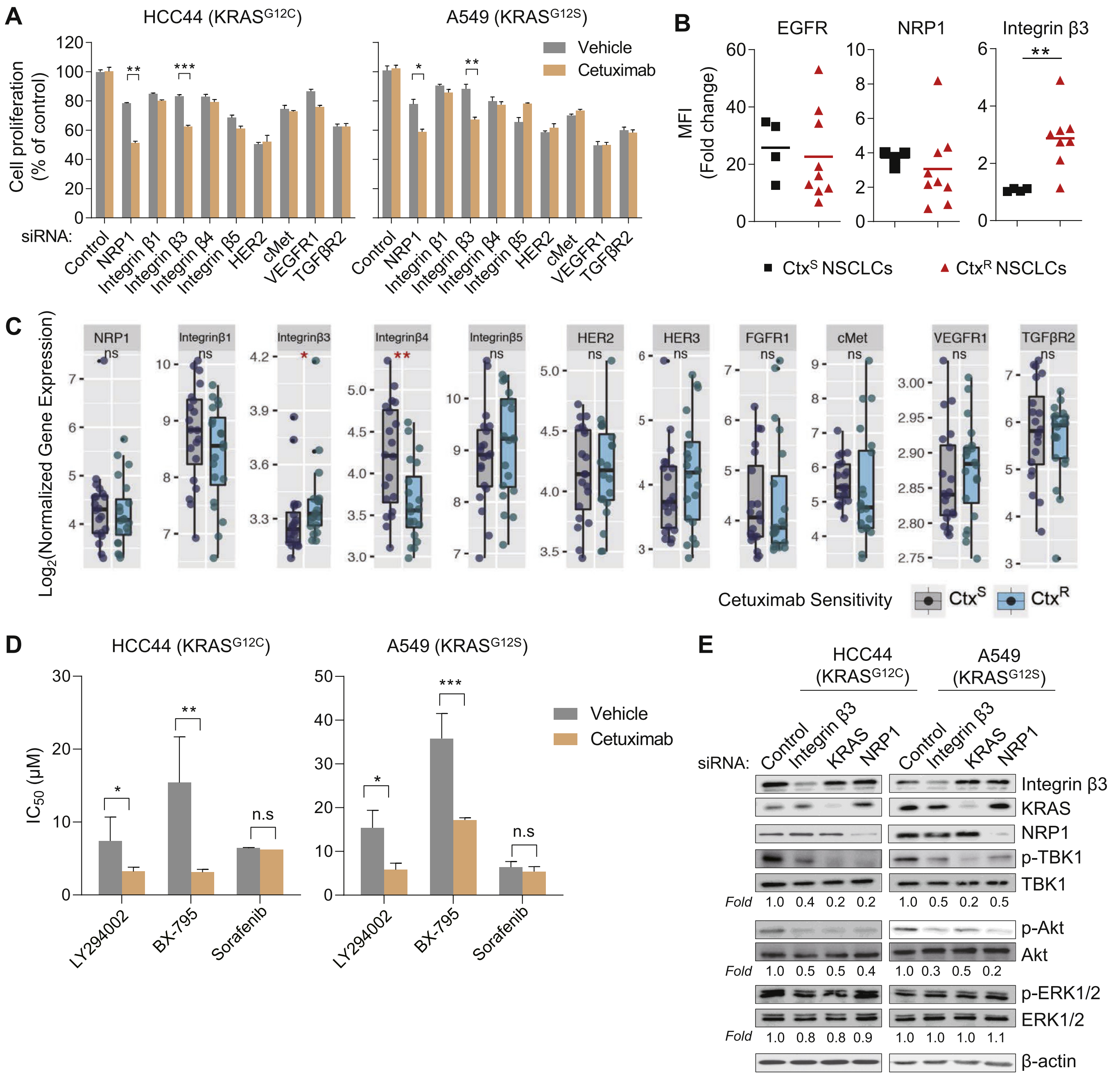

Fig. 2. Integrin β3 expression is associated with cetuximab resistance in KRAS^{MUT} NSCLCs. (**A**) Effects of knockdown of the indicated gene by siRNA on sensitivity to cetuximab treatment (2 μM) for 48 h, as assessed by cell proliferation assays. Error bars, ± SD (n = 3). $^*P < 0.05$, $^{**}P < 0.01$, $^{***}P < 0.001$; n.s., not significant. (**B**) Comparisons of cell surface expression levels of EGFR, NRP1, and integrin β3 between Ctx^S and Ctx^R NSCLCs, analyzed by flow cytometry as shown in Supplementary Figs. S1A and S5 and then quantified by mean fluorescence intensity (MFI). (**C**) Box plots of mRNA expression levels of indicated genes according to Ctx^S or Ctx^R status in lung adenocarcinoma (LUAC) cell lines, retrieved from the Genomics of Drug Sensitivity in Cancer database. $^*P < 0.05$, $^{**}P < 0.01$ (Wilcoxon rank sum test). (**D**) IC$_{50}$ values of the indicated pharmacological inhibitor with or without cetuximab (2 μM), determined after treatment of the cell lines for 48 h. The dose-dependent inhibition of cell proliferation by each inhibitor with or without cetuximab and their IC$_{50}$ values are shown in Supplementary Fig. S6. Error bars, ± SD (n = 3). $^*P < 0.05$, $^{**}P < 0.01$, $^{***}P < 0.001$; n.s., not significant. (**E**) Effects of knockdown of indicated gene by siRNA on KRAS downstream signaling including Akt, TBK1, and ERK1/2, as measured by western blotting. The number below the panel indicates the relative value of band intensity of phosphorylated proteins compared to band intensity in the 'control siRNA' group after normalization to the band intensity of respective total protein for each sample.

2.8. Statistical analysis

Data represent the mean ± SD of triplicate samples from one representative experiment based on at least three independent experiments, unless otherwise specified. Unpaired two-tailed student's *t* tests were used to evaluate the significance of differences between two groups, and one-way ANOVA with the Newman-Keuls post hoc test was used to evaluate differences among three or more groups using GraphPad Prism 5 software (GraphPad). Differences between samples were considered statistically significant at $P < 0.05$.

3. Results

3.1. EGFR/NRP1 dual-targeting inhibits the proliferation of KRAS^{MUT} NSCLCs

To examine whether Ctx-TPP11 (Fig. 1A) can inhibit KRAS^{MUT} NSCLCs, we assessed the *in vitro* anti-proliferation effects of Ctx-TPP11 alone or combination of cetuximab and Fc-TPP11 using a panel of cetuximab-sensitive (Ctx^{S}), wild-type RAS (Ctx^{S}/RAS^{WT}), and cetuximab-resistant (Ctx^{R}), RAS^{MUT} (Ctx^{R}/RAS^{MUT}) NSCLCs with different KRAS or NRAS mutation subtypes (Supplementary Table S1). Ctx-TPP11 alone or combination of cetuximab and Fc-TPP11 effectively inhibited the proliferation of both Ctx^{S}/RAS^{WT} and Ctx^{R}/RAS^{MUT} NSCLCs, as compared to that with cetuximab alone, which was only effective against Ctx^{S}/RAS^{WT} NSCLCs (Fig. 1B). Notably, Ctx^{R}/KRAS^{MUT} HCC2108 and H460 cells, lacking detectable NRP1 expression on the cell surface (Supplementary Fig. S1A), displayed negligible sensitivity to Ctx-TPP11 and the combination. NRP1 knockdown via small interfering RNA (siRNA) transfection (Supplementary Fig. S1B) resulted in a 20–25% decrease in the proliferation of Ctx^{R}/KRAS^{MUT} cells and abolished the superior anti-proliferation effects of Ctx-TPP11 on Ctx^{R}/KRAS^{MUT} cells (Fig. 1C). These results indicated that NRP1 expression contributes to Ctx^{R}/KRAS^{MUT} cell proliferation and is a prerequisite to sensitize Ctx^{R}/KRAS^{MUT} cells to Ctx-TPP11.

To further assess whether fusions of TPP11 and other EGFR-targeting Abs could sensitize Ctx^{R}/KRAS^{MUT} NSCLCs, we generated EGFR/NRP1 dual-targeting bsAbs in the IgG-TPP11 format using necitumumab, nimotuzumab, and matuzumab (Supplementary Figs. S2A and B). For combination treatment with chemotherapy for advanced NSCLC, necitumumab has been approved and nimotuzumab and matuzumab are now in clinical trials [24,25]. Like Ctx-TPP11, all three anti-EGFR IgG-TPP11 bsAbs substantially inhibited the proliferation of Ctx^{R}/KRAS^{MUT} NSCLCs, but not Ctx^{S}/RAS^{WT} NSCLCs, compared to that with parental Abs (Fig. 1D; Supplementary Fig. S2B). These results demonstrated that co-targeting EGFR and NRP1 can attenuate the resistance of KRAS^{MUT} NSCLCs to EGFR-targeted Ab treatment.

We further examined combination effects of Fc-TPP11 with EGFR TKI erlotinib or pan-ERBB TKI afatinib [26] on RAS^{MUT} NSCLCs. While Ctx^{S}/RAS^{WT} PC-9 cells were sensitive to both erlotinib and afatinib, the tested Ctx^{R}/RAS^{MUT} NSCLCs were largely resistant to the single-agent treatments (Supplementary Fig. S3A). The combination of each TKI with Fc-TPP11 did not improve the efficacy against the TKI-sensitive Ctx^{S}/RAS^{WT} PC-9 cells, but significantly sensitized the TKI-resistant Ctx^{R}/RAS^{MUT} HCC44, H1299, and A549 cells (Fig. 1E; Supplementary Fig. S3B). However, the combined effects were not observed for NRP1-negative Ctx^{R}/KRAS^{MUT} HCC2108 and H460 cells. These results suggested that Fc-TPP11-mediated NRP1 targeting can attenuate the resistance of RAS^{MUT} NSCLCs to EGFR-TKI or pan-ERBB TKI treatment. Of note, combined treatment with the pan-ERBB TKI afatinib and Fc-TPP11 exhibited more substantial growth inhibition of the NRP1-positive Ctx^{R}/RAS^{MUT} NSCLCs compared to the EGFR TKI erlotinib + Fc-TPP11 combination (Fig. 1E; Supplementary Fig. S3B). These findings suggested that combination of NRP1-targeting Fc-TPP11 with pan-ERBB TKI is a more effective strategy against RAS^{MUT} NSCLCs than the combination with EGFR-TKI [26].

3.2. Integrin β3 expression is associated with the intrinsic resistance of KRAS^{MUT} NSCLCs to cetuximab

NRP1 bilaterally interacts with many other transmembrane signaling receptors [17,18]. To elucidate which receptor(s) is involved in the sensitization of KRAS^{MUT} NSCLC to Ctx-TPP11, we evaluated cetuximab sensitivity after knocking down NRP1-interacting receptors using specific siRNA (Supplementary Fig. S4A). The knockdown of integrin β1, β4, or β5, HER2, cMet, VEGFR1, or TGFβR2 failed to sensitize Ctx^{R}/KRAS^{MUT} cells to cetuximab (Fig. 2A). In contrast, the depletion of either NRP1 or integrin β3 resulted in increased sensitivity to cetuximab for all five Ctx^{R}/KRAS^{MUT} NSCLCs tested (Fig. 2A; Supplementary Fig. S4B), suggesting that NRP1 and integrin β3 expression is associated with cetuximab resistance in KRAS^{MUT} NSCLCs.

To further clarify the role of both NRP1 and integrin β3 in Ctx^{R}/KRAS^{MUT} NSCLCs, we compared baseline expression levels of NRP1 and integrin β3, as well as EGFR and integrin β1, between Ctx^{S}/RAS^{WT} and Ctx^{R}/KRAS^{MUT} NSCLCs by flow cytometry (Supplementary Figs. S1A and S5). We observed little correlation between basal expression levels of EGFR, NRP1, or integrin β1 and cetuximab sensitivity. However, Ctx^{R}/KRAS^{MUT} NSCLCs exhibited higher cell surface expression levels of integrin β3 than Ctx^{S}/RAS^{WT} NSCLCs, which displayed negligible expression of integrin β3 (Fig. 2B). This result indicated that cell-surface integrin β3 expression is associated with cetuximab resistance in KRAS^{MUT} NSCLCs.

From the GDSC database [23], we procured mRNA expression levels of NRP1-interacting receptors in Fig. 2A along with the IC$_{50}$ values (drug concentration that reduces viability by 50%) of cetuximab for 40 lung adenocarcinoma (LUAC) cell lines, and then compared Ctx^{S} and Ctx^{R} groups. We further examined the expression levels of the receptors, ERBB3/HER3 and FGFR1, which have been reported to be implicated in the resistance of KRAS^{MUT} NSCLCs to EGFR-targeted therapy [27,28]. Noticeably, we observed the significant mRNA upregulation of integrin β3 in Ctx^{R} LUAC cell lines ($p = 0.01954$), whereas the other receptors were not differentially expressed, except for integrin β4, which was significantly downregulated in Ctx^{R} LUAC groups (Fig. 2C). This result further supports the widespread association between integrin β3 expression and cetuximab resistance in NSCLCs.

3.3. PI3K-Akt and RalB-TBK1 pathways are associated with integrin β3-mediated cetuximab resistance in KRAS^{MUT} NSCLCs

KRAS^{MUT} can activate many downstream effectors including the most prominent Raf-MEK-ERK, PI3K-Akt, and RalB-TBK1 pathways [12]. To determine which pathways are involved in integrin β3-mediated cetuximab resistance of KRAS^{MUT} NSCLCs, we investigated the dose-dependent inhibition of cell proliferation in HCC44 and A549 cells by pharmacological inhibitors including Raf/MEK inhibitors (sorafenib, trametinib, and RO5126766), PI3K inhibitors (LY294002, pictilisib, and buparlisib), and TBK1 inhibitor (BX-795) as a single agent as well as the combination with cetuximab (2 μM). The presence of cetuximab significantly enhanced suppression of cell proliferation by the PI3K inhibitors and TBK1 inhibitor lowering the IC$_{50}$ values compared to those of each inhibitor alone in the two cells (Fig. 2D; Supplementary Fig. S6). However, no additional effect was observed for the Raf/MEK inhibitors combined with cetuximab. These data implied that the PI3K and TBK1 pathways, but not Raf-MEK-ERK pathway, are associated with cetuximab resistance in KRAS^{MUT} NSCLCs.

Next, we examined whether integrin β3 and NRP1 are involved in the activation of KRAS downstream pathways using gene silencing in Ctx^{R}/KRAS^{MUT} HCC44 and A549 NSCLCs. The activation of Akt and TBK1 was attenuated after integrin β3, NRP1, or KRAS^{MUT} knockdown in these cells (Fig. 2E). However, activation of the Raf-MEK-ERK pathway was not affected. Together, these results suggest that the PI3K-Akt and RalB-TBK1 pathways, but not Raf-MEK-ERK, comprise downstream signaling axes involved in cetuximab resistance in KRAS^{MUT} NSCLCs.

3.4. Integrin β3 mediates the formation of a NRP1–integrin β3–KRAS^{MUT} ternary complex

Integrin β3 has been reported to drive EGFR TKI resistance in KRAS^{MUT} NSCLCs and PDACs by forming an integrin β3–KRAS^{MUT} complex, thereby activating downstream signaling, mainly comprising the RalB-TBK1 pathway [10]. In a separate study, integrin β3 was also documented to interact with NRP1 in VEGF-stimulated endothelial cells

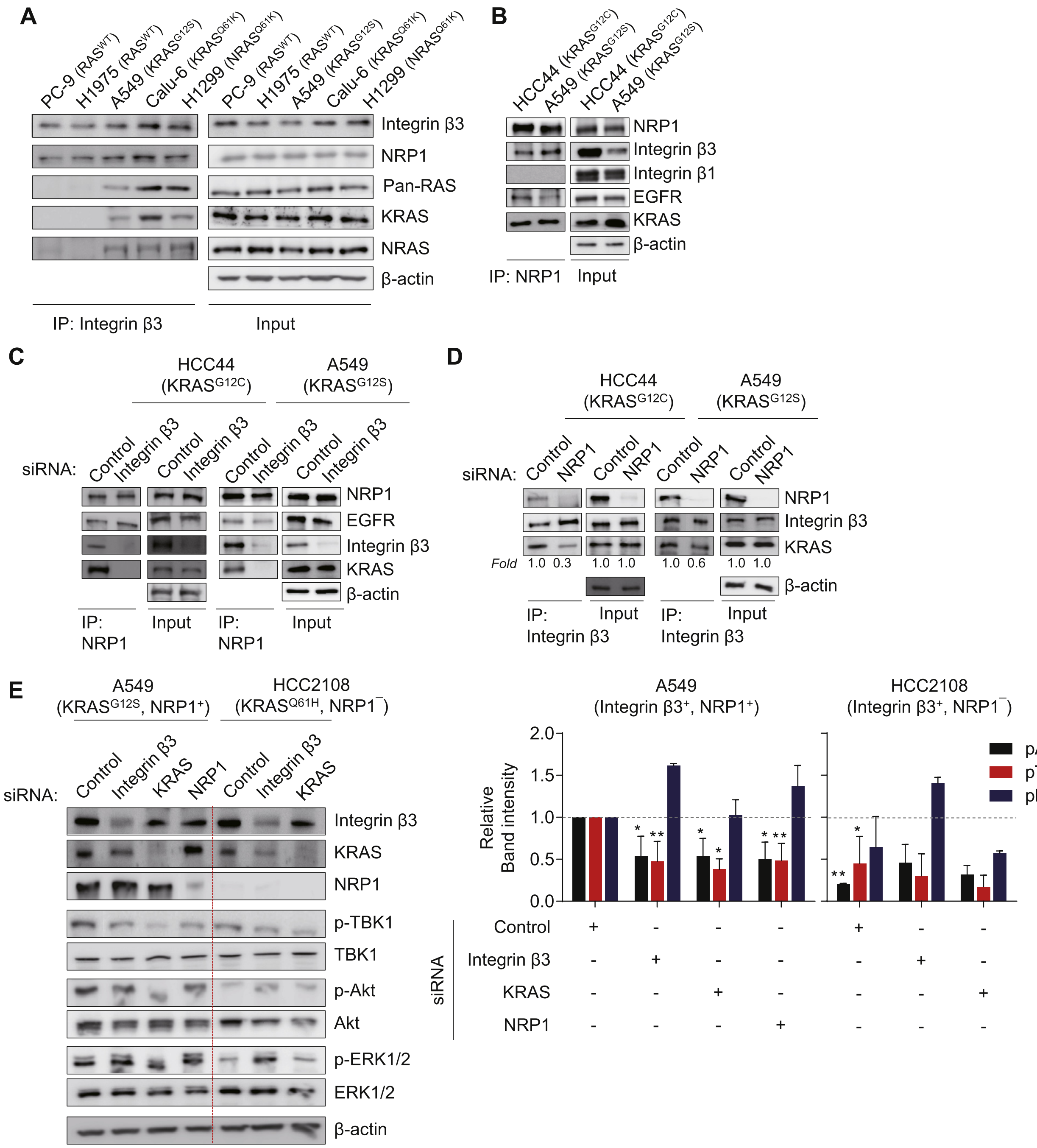

Fig. 3. Integrin β3 mediates the formation of NRP1–integrin β3–KRAS^{MUT} ternary complexes in KRAS^{MUT} NSCLCs. (**A, B**) Immunoprecipitation (IP) of indicated proteins with integrin β3 (A) and NRP1 (B) in NSCLCs. (**C, D**) IP of indicated proteins with NRP1 after siRNA-mediated knockdown of integrin β3 (C) and with integrin β3 after siRNA-mediated knockdown of NRP1 (D) in the cells. (**E**) Representative immunoblots showing the levels of pAkt, pTBK1, and pERK1/2 in A549 and HCC2108 cells after knockdown of the indicated gene by siRNA. The right panel shows the relative band intensity of the indicated phosphoprotein compared to that of the control band in A549 cells. Error bars, ± SD (n = 3). $*P < 0.05$, $**P < 0.01$ versus control band of A549 cells.

[29]. To identify any possible physical interactions between integrin β3 and NRP1 and/or RAS in the context of RAS mutation status, we performed immunoprecipitation experiments using well-validated anti-RAS antibodies in terms of their selectivity and sensitivity to RAS isoforms and mutation subtypes [30]. Whereas integrin β3 was co-precipitated with NRP1 in both RAS^{WT} and RAS^{MUT} NSCLCs tested, it bound RAS^{MUT} in only KRAS^{MUT} or NRAS^{MUT} NSCLCs, and not RAS^{WT} in RAS^{WT} NSCLCs (Fig. 3A). Based on NRP1-pulldown assays, NRP1 was co-precipitated with both integrin β3 and KRAS^{MUT}, but not integrin β1, in Ctx^{R}/KRAS^{MUT} cells (Fig. 3B). Together, these results suggested that integrin β3 constitutively interacts with NRP1 and that the NRP1–integrin β3 complex selectively interacts with RAS^{MUT}, but not with RAS^{WT}, to form a NRP1–integrin β3–RAS^{MUT} ternary complex only in RAS^{MUT} NSCLCs. This finding suggested that the ability of KRAS^{MUT} to drive cetuximab resistance is linked to its assembly with integrin β3 and NRP1. Since there are no obvious RAS-binding sites in the cytoplasmic domain of NRP1 [17], we reasoned that integrin β3 might serve as an intermediary adaptor that facilitates the formation of NRP1–integrin β3-RAS^{MUT} complexes. Indeed, knockdown of integrin β3 in HCC44 and A549 cells abolished the co-precipitation of KRAS^{MUT} after NRP1 pulldown (Fig. 3C), indicating the absence of interactions between NRP1 and KRAS^{MUT} without integrin β3. However, integrin β3

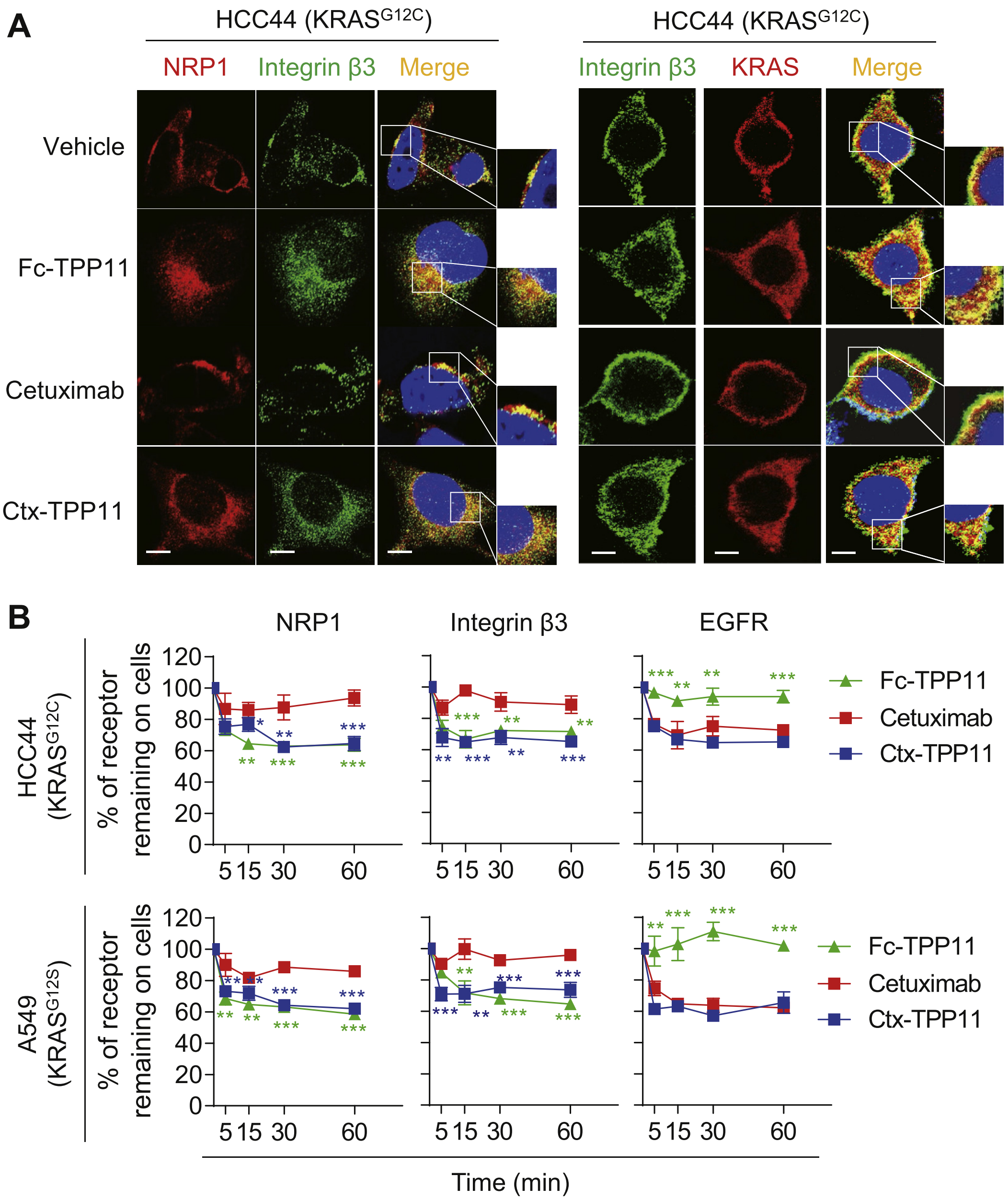

Fig. 4. Ctx-TPP11 downregulates plasma membrane levels of the NRP1–integrin β3–KRAS^{MUT} ternary complex via NRP1-coupled internalization. (A) Representative confocal microscopy images showing co-localization of NRP1 with integrin β3 (left) and integrin β3 with KRAS^{MUT} (right) in HCC44 cells treated with indicated agents (2 μM) for 1 h at 37 °C before analysis. More than 10 cells for each group were analyzed. **(B)** Flow cytometric analysis of remaining cell surface levels of NRP1, integrin β3, and EGFR in HCC44 and A549 cells, treated with agents for the indicated times at 37 °C. Approximately 10,000 cells were collected and analyzed by FlowJo V10 software (Tree Star). The mean fluorescent intensities (MFIs), normalized to that in untreated control cells under each experimental condition, are plotted from triplicate experiments. The representative histograms are shown in Supplementary Fig. S7B. Error bars, ± SD (n = 3). $^{*}P < 0.05$, $^{**}P < 0.01$, $^{***}P < 0.001$ versus cetuximab-treated cells.

pulldown in NRP1-depleted cells was found to result in the co-precipitation of KRAS^{MUT}, but the amount was substantially reduced (Fig. 3D). This suggests that NRP1 is not essential for integrin β3–KRAS^{MUT} interactions, but promotes and/or stabilizes these complexes. Immunoprecipitation of NRP1 also co-precipitated EGFR in HCC44 and A549 cells (Fig. 3B and C), consistent with a previous result [31]. Nevertheless, it seemed that EGFR is not substantially involved in the NRP1–integrin β3-RAS^{MUT} complex because cetuximab alone failed to sensitize those cells (Fig. 1B).

To further determine the role of NRP1 in NRP1–integrin β3–KRAS^{MUT}-mediated signaling, we compared KRAS^{MUT} downstream signaling between NRP1-positive A549 and NRP1-negative HCC2108 cells. The basal activation levels of pAkt and pTBK1 were much higher in A549 than in HCC2108 cells (Fig. 3E). Integrin β3, NRP1, or KRAS^{MUT} knockdown substantially reduced the amount of pAkt and pTBK1 to a similar extent only in NRP1-positive A549 cells, without decreasing pERK levels. These results demonstrated that each component of the ternary complex is equally essential for downstream signaling.

3.5. Ctx-TPP11 downregulates cell surface levels of the integrin β3–KRAS^{MUT} complex via NRP1-coupled internalization

Confocal fluorescence microscopy studies revealed that during steady-state Ctx^{R}/KRAS^{MUT} conditions in HCC44 and A549 cells, integrin β3 co-localized with NRP1 and KRAS^{MUT} on the plasma

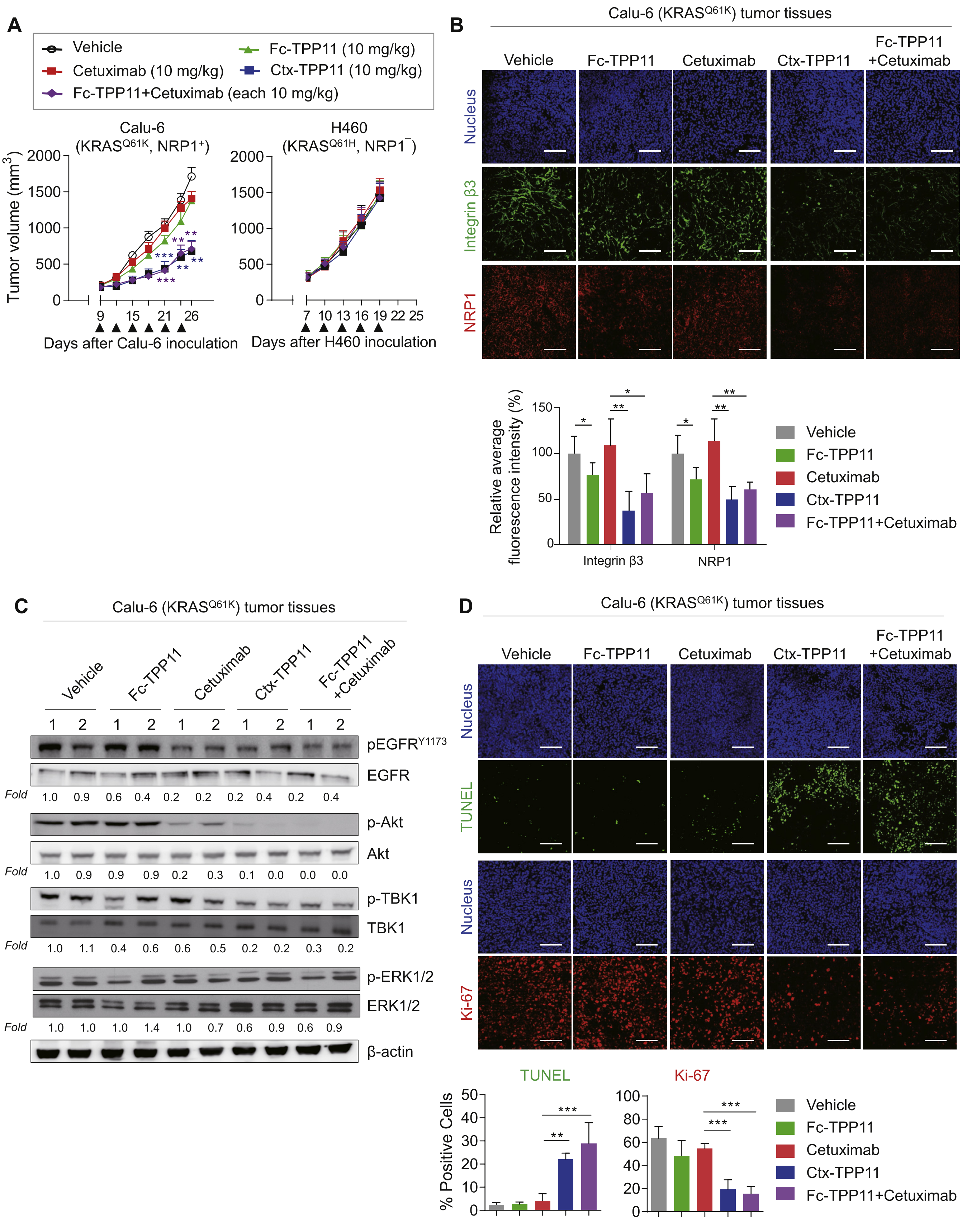

(caption on next page)

Fig. 5. Co-targeting of EGFR and NRP1 suppresses *in vivo* growth of Ctx^{R}/KRAS^{MUT} NSCLC CDXs in a mouse model. (A) Tumor growth was analyzed by measuring tumor volume during treatment with indicated agents in female BALB/c nude mice harboring pre-established Calu-6 or H460 CDXs. Fc-TPP11, cetuximab, or Ctx-TPP11 were intravenously dosed at 10 mg/kg every 3 days (▲). Error bars, ± SD (n = 6 per group). $^{**}P < 0.01$, $^{***}P < 0.001$ versus cetuximab-treated cells. (**B–D**) Representative immunohistofluorescence images showing the levels of integrin β3 and NRP1 (B), immunoblots examining the activation levels of pEGFR (Y1173), pAkt (S473), pTBK1 (S172), and pERK1/2 (T202/Y204) (C), and representative immunohistofluorescence images showing TUNEL and Ki-67 staining (D) in Calu-6 tumors excised from mice at the end of treatment as in (A). In (B and D), nuclei were counterstained with Hoechst 33342 (blue). In (B), the lower panel shows the percent relative fluorescence intensity compared to that in the vehicle-treated control group after normalization to the nuclei staining (n ≥ 200 cells per image). Scale bars, 100 μm $^{*}P < 0.05$, $^{**}P < 0.01$. In (C), two independent tumor tissue samples, indicated as 1 and 2, were analyzed. In (D), the lower panels show the percentage of TUNEL- and Ki-67-positive cells compared to the number of Hoechst 33342-stained cells (n ≥ 250 cells per image) for each sample. Error bars represent the mean ± SD of six random fields for each immunohistofluorescence sample (n = 2 tumors per group). $^{**}P < 0.01$, $^{***}P < 0.001$. In (A, B, and D), statistical analysis was performed using a one-way analysis of variance followed by the Newman-Keuls post-hoc test.

membrane (Fig. 4A; Supplementary Fig. S7A), corroborating the immunoprecipitation results of the NRP1–integrin β3–KRAS^{MUT} ternary complex (Fig. 3). However, upon treatment with Ctx-TPP11 or Fc-TPP11, NRP1/integrin β3 and integrin β3/KRAS^{MUT} were detected together in the cytoplasmic compartment, with a concomitant decrease in cell surface levels of integrin β3 and KRAS^{MUT} (Fig. 4A; Supplementary Fig. S7A). Time-course analysis revealed that the cell surface levels of both NRP1 and integrin β3 were rapidly reduced within 15 min upon Fc-TPP11 or Ctx-TPP11, but not by cetuximab, treatment in the two cell lines (Fig. 4B; Supplementary Fig. S7B). These results demonstrated that Ctx-TPP11- or Fc-TPP11-mediated NRP1 endocytosis induces the co-internalization of integrin β3 and KRAS^{MUT} due to their physical interactions in the ternary complex, resulting in the downregulation of integrin β3 and KRAS^{MUT}. Further, these findings indicated that Ctx-TPP11 can sensitize KRAS^{MUT} NSCLCs by downregulating the NRP1–integrin β3–KRAS^{MUT} ternary complex, thereby attenuating signaling through this complex that mediates cetuximab resistance. The cell surface levels of EGFR were significantly reduced by treatment with cetuximab or Ctx-TPP11, but negligibly by Fc-TPP11 treatment (Fig. 4B; Supplementary Fig. S7B). These results, along with the negligible downregulation of NRP1 and integrin β3 by cetuximab treatment, implied that the association of endogenous NRP1 with EGFR (Fig. 3B) is too weak to trigger the NRP1-coupled co-internalization of EGFR at the steady-state.

3.6. *Ctx-TPP11 exhibits in vivo anti-tumor efficacy against KRAS^{MUT} NSCLC CDX tumors*

We next evaluated the *in vivo* anti-tumor efficacy of Ctx-TPP11 in nude mice bearing established NRP1-positive Calu-6 and NRP1-negative H460 Ctx^{R}/KRAS^{MUT} NSCLC CDX tumors. Consistent with *in vitro* findings, Ctx-TPP11 significantly slowed down the growth of Calu-6 tumor xenografts, resulting in ~59% increased TGI (Fig. 5A) and an approximate 62% greater reduction in tumor weight, compared to those in cetuximab or Fc-TPP11 only groups (Supplementary Figs. S8A and B). The combined treatment of cetuximab and Fc-TPP11 yielded similar *in vivo* anti-tumor efficacy to that of Ctx-TPP11. However, for NRP1-negative H460 tumors, Ctx-TPP11 alone and combined treatment did not exhibit any enhanced anti-tumor efficacy compared to that with cetuximab alone and vehicle treatment (Fig. 5A; Supplementary Figs. S8A and B). The body weights of mice, monitored as an indicator of antibody toxicity, were also similar between the treatment groups (Supplementary Fig. S8C).

An examination of excised Calu-6 tumor tissues after treatment with Ctx-TPP11, Fc-TPP11, or combined cetuximab plus Fc-TPP11 showed the downregulation of NRP1 and integrin β3 compared to those in vehicle- and cetuximab-treated tumor tissues (Fig. 5B). This suggests that NRP1 internalization, mediated by the bivalent TPP11 moiety, triggers the co-internalization of integrin β3 for lysosomal degradation, consistent with *in vitro* results (Fig. 4). Moreover, compared to those in vehicle-, Fc-TPP11-, and cetuximab-treated tumor tissues, Ctx-TPP11- and combination-treated tumor tissues showed significantly reduced levels in KRAS^{MUT} downstream Ctx^{R} signaling including pAkt and pTBK1 (Fig. 5C), increased apoptosis as measured by terminal deoxynucleotidyl transferase dUTP nick end labeling (TUNEL)-staining, and decreased proliferation as evidenced by staining for the cell proliferation marker Ki-67 (Fig. 5D) [11,15]. Together, these results demonstrated that Ctx-TPP11 can sensitize KRAS^{MUT} NSCLC to cetuximab by attenuating Ctx^{R} signaling induced by NRP1–integrin β3–KRAS ternary complex formation, consistent with *in vitro* results.

3.7. *Ctx-TPP11 displays potent anti-tumor activity in KRAS^{MUT} NSCLC PDX tumors*

To further demonstrate the therapeutic efficacy of Ctx-TPP11, we established two PDXs from patients with KRAS^{MUT} NSCLC, YHIM-1010 (KRAS^{G12C}) and YHIM-1031 (KRAS^{G12R}) (Supplementary Table S2). Despite EGFR expression, the two models were resistant to cetuximab alone (Fig. 6A). Notably, however, Ctx-TPP11 significantly retarded the growth of both PDXs compared to that with cetuximab treatment with TGI of ~54% and ~47% for YHIM-1010 and YHIM-1031, respectively. Compared to those in vehicle-treated tumor tissues, both cetuximab- and Ctx-TPP11-treated tumor tissues showed significantly reduced levels of phosphorylated EGFR (Fig. 6B). However, Ctx-TPP11 treatment, but not cetuximab, resulted in the substantial downregulation of NRP1 and integrin β3 (Fig. 6B), suggesting that it can induce the degradation of both NRP1 and integrin β3 via NRP1-coupled cellular internalization due to the formation of this complex in patient-derived NSCLC. Further, Ctx-TPP11-treated tumor tissues displayed increased apoptosis as assessed by TUNEL and Ki-67 staining results (Fig. 6C), explaining the anti-tumor activity of Ctx-TPP11. During antibody treatments, the mice did not exhibit any significant body weight loss (Supplementary Fig. S9). These results demonstrate that Ctx-TPP11 attenuates cetuximab resistance in KRAS^{MUT} NSCLC PDX models through similar mechanisms observed in CDX models.

4. Discussion

Although *KRAS* is the most frequent oncogene in NSCLC, no effective therapy is currently available for KRAS^{MUT} NSCLC patients [6,7,24]. In this study, we showed that integrin β3 expression is associated with the intrinsic resistance of KRAS^{MUT} NSCLCs to anti-EGFR Ab cetuximab. Further analyses identified integrin β3-mediated NRP1–integrin β3–KRAS^{MUT} complex formation and its downstream signaling components PI3K-Akt and RalB-TBK1 as a primary cetuximab resistance mechanism of KRAS^{MUT} NSCLC. We further demonstrated that the dual-targeting of EGFR/NRP1 by the Ctx-TPP11 bsAb can attenuate cetuximab resistance in KRAS^{MUT} NSCLC *in vitro* and *in vivo*, including in PDX models, regardless of the specific KRAS mutational subtypes examined. Moreover, the blockade of EGFR with the cetuximab moiety results in inactivation of the ligand-dependent pathway, whereas the downregulation of NRP1 with the bivalent Fc-TPP11 moiety causes the inactivation of ligand-independent NRP1–integrin β3–KRAS^{MUT}-driven bypass signaling through PI3K-Akt and RalB-TBK1. Our results document that NRP1 is a potential target to attenuate NRP1–integrin β3–KRAS^{MUT} signaling for the treatment of KRAS^{MUT} NSCLC.

Integrins, main cellular adhesion receptors, have many functions and are often implicated as a driver of resistance to anti-cancer

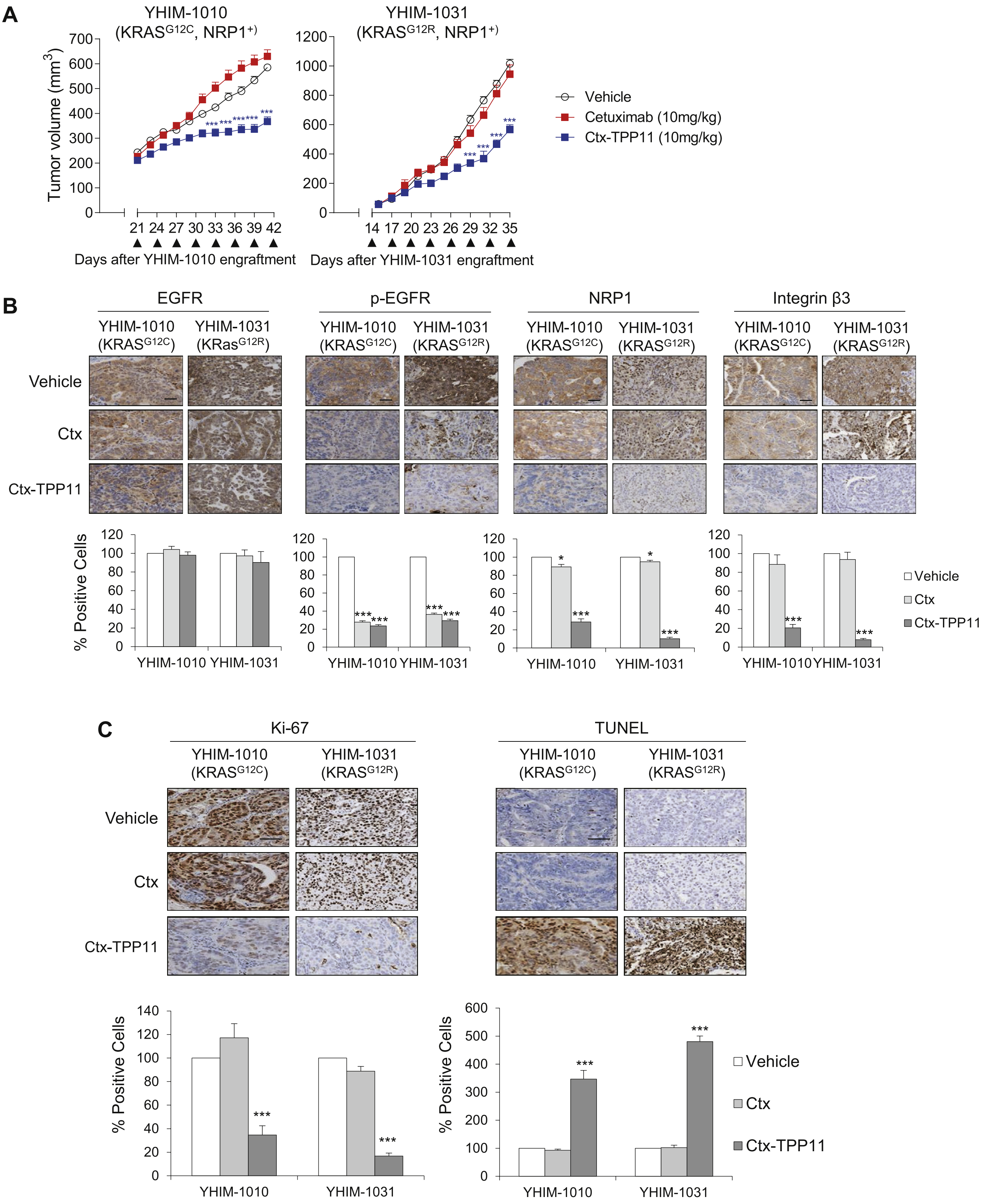

Fig. 6. CTX-TPP11 reduces the *in vivo* growth of Ctx^R/KRAS^{MUT} NSCLC PDXs. (**A**) Tumor growth of two KRAS^{MUT} NSCLC PDXs during treatment with indicated agents. Cetuximab and Ctx-TPP11 were intraperitoneally dosed at 10 mg/kg every 3 days (▲). Error bars, ± SD (n = 5 per group). ***$P < 0.001$ versus cetuximab-treated cells. (**B**) Representative immunohistochemical images showing the levels of EGFR, pEGFR (Y1173), NRP1, and integrin β3. (**C**) Representative immunohistochemical images showing Ki-67 and TUNEL staining. In (B and C), tumor tissues excised from mice at the end of treatment were analyzed and the panels show the percent positive cells compared to that in the vehicle-treated control group. Error bars represent the mean ± SD of six random fields for each immunohistochemical sample (n = 2 tumors per group). *$P < 0.05$, ***$P < 0.001$ versus vehicle-treated control. Scale bars, 100 μm. In (B–C), Ctx, Cetuximab.

therapeutics [32]. Several integrins such as integrin β1, β4, and β5 are highly expressed in NSCLC, but integrin β3, usually expressed in the endothelium of blood vessels, is also expressed in approximately one-third of NSCLCs [33]. Recent studies have shown that integrin β3 expression promotes tumor progression and metastasis [34] and recruits $KRAS^{MUT}$ to the cancer cell plasma membrane to form integrin β3–$KRAS^{MUT}$ complexes in NSCLCs, which leads to downstream RalB-TBK1 signaling, facilitating resistance to EGFR TKIs [10]. In our study, we identified for the first time that NRP1 interacts with integrin β3–$KRAS^{MUT}$ to form an NRP1–integrin β3–$KRAS^{MUT}$ ternary complex in $KRAS^{MUT}$ NSCLCs, where integrin β3 serves as an intermediary adaptor and NRP1 facilitates ternary complex formation (Figs. 3 and 4). Even though a previous study reported that integrin β3 physically interacts with $KRAS^{MUT}$ [10], they did not determine whether integrin β3 interacts with other RAS^{MUT} variants or RAS^{WT}. Importantly, we found that integrin β3 associates only with RAS^{MUT} variants, such as $KRAS^{MUT}$ and $NRAS^{MUT}$, but not RAS^{WT}, suggesting that RAS^{MUT} modulates the role of integrin β3 and NRP1 in $KRAS^{MUT}$ NSCLC. The knockdown of either NRP1 or integrin β3 sensitized $KRAS^{MUT}$ NSCLCs to cetuximab treatment through a molecular mechanism including the suppression of PI3K-Akt and RalB-TBK1 signaling downstream of the NRP1–integrin β3–$KRAS^{MUT}$ complex (Figs. 2 and 3). However, the Raf-MEK-ERK pathway was neither associated with cetuximab resistance nor affected by NRP1 or integrin β3 knockdown. A recent report using an irreversible inhibitor of $KRAS^{G12C}$ also showed that combinations with a PI3K inhibitor, but not a MEK inhibitor, were effective for $KRAS^{G12C}$ NSCLC [35]. Together, these results provide a strong rationale for clinical trials to investigate integrin β3 expression and downstream PI3K-Akt and RalB-TBK1 signaling through the NRP1–integrin β3–$KRAS^{MUT}$ complex, rather than KRAS mutation status alone, as more suitable predictive biomarkers of cetuximab resistance in $KRAS^{MUT}$ NSCLC.

The overexpression of NRP1 observed in many solid cancers including NSCLC has been reported to be associated with NSCLC radioresistance [19], tumor progression, and poor outcome through the PI3K-Akt pathway [20,31]. Drug resistance signaling via the coupling of NRP1 with integrins such as β1, β3, and β4 has also been documented [15,36,37]. We previously identified NRP1-coupled active integrin β1-driven Src-Akt bypass signaling as a primary cetuximab resistance mechanism in PDACs [15]. Interestingly, NRP1 was found to selectively interact with integrin β3, but not integrin β1, in $KRAS^{MUT}$ NSCLCs (Fig. 3B). It is unclear why this selectivity is different according to the tumor type. However, it is likely due to different expression levels of active integrin β1 and integrin β3 between PDACs and NSCLCs. Specifically, NSCLCs expressed more integrin β3, but much less active integrin β1, than PDACs (Supplementary Fig. S5).

In $KRAS^{MUT}$ NSCLCs, we found that NRP1 knockdown or addition of the NRP1-targeting agent, Fc-TPP11, sensitized cells to cetuximab. The bivalent engagement of NRP1 by Fc-TPP11 or Ctx-TPP11 efficiently triggered cellular internalization, which also induced the co-internalization of integrin β3 and $KRAS^{MUT}$ due to their physical interactions with NRP1 on the cell surface (Figs. 3 and 4). Given that endocytosed NRP1 and integrin β3 are degraded in lysosomes [38,39], the co-internalized $KRAS^{MUT}$ was suggested to be degraded in lysosomes. This resulted in the attenuation of NRP1–integrin β3–$KRAS^{MUT}$ downstream signaling, eventually sensitizing $KRAS^{MUT}$ NSCLCs to cetuximab. This highlights the potential of targeting NRP1 as a therapeutic strategy to disrupt integrin β3–$KRAS^{MUT}$-mediated PI3K-Akt and RalB-TBK1 signaling in $KRAS^{MUT}$ NSCLC.

In conclusion, our results show that integrin β3-mediated NRP1–integrin β3–$KRAS^{MUT}$ complex formation is implicated in the intrinsic cetuximab resistance mechanism of $KRAS^{MUT}$ NSCLC. Our study also demonstrates that NRP1 targeting by Ctx-TPP11 can attenuate Ctx^{R} signaling by downregulating cell surface levels of the NRP1–integrin β3–$KRAS^{MUT}$ complex through NRP1-coupled internalization. Our work suggests that concurrent targeting of EGFR/NRP1 by the Ctx-TPP11 bsAb might be an effective clinical strategy to circumvent the resistance of $KRAS^{MUT}$ NSCLC to EGFR-targeted therapy.

Authors' contributions

Y.S.K. and Y.J.K. conceived the idea and designed the experiments. Y.J.K., D.S.B., and S.L. purified antibodies and performed *in vitro* cellular and *in vivo* CDX experiments. H.N.K. and B.C.C. performed PDX experiments. D.P. analyzed GDSC database. All authors analyzed and interpreted data. Y.S.K. and B.C.C. supervised the research. Y.S.K., Y.J.K. and B.C.C. wrote the manuscript with input from all co-authors. All authors approved the final version.

Conflicts of interest

Y.S.K. and Y.J.K. are inventors on a patent application related to the bispecific antibody described in this work. All other authors declare no potential conflicts of interest.

Acknowledgements

The authors would like to thank Ji-Sun Kim and Dr. Keunok Jung for their experimental assistance with the manuscript. This work was supported by the National Research Foundation (NRF) Grant (2014M3C1A3051470 and 2016R1A2A2A05005108 to YSK and 2016R1A2B3016282 to BCC) funded by the Ministry of Science, ICT & Future Planning, Republic of Korea.

Appendix A. Supplementary data

Supplementary data to this article can be found online at https://doi.org/10.1016/j.canlet.2019.09.005.

References

[1] L. Crino, W. Weder, J. van Meerbeeck, E. Felip, E.G.W. Group, Early stage and locally advanced (non-metastatic) non-small-cell lung cancer: ESMO Clinical Practice Guidelines for diagnosis, treatment and follow-up, Ann. Oncol. 21 (Suppl 5) (2010) v103–115.

[2] J. Brabender, K.D. Danenberg, R. Metzger, P.M. Schneider, J. Park, D. Salonga, A.H. Holscher, P.V. Danenberg, Epidermal growth factor receptor and HER2-neu mRNA expression in non-small cell lung cancer Is correlated with survival, Clin. Cancer Res. 7 (2001) 1850–1855.

[3] N. Thatcher, F.R. Hirsch, A.V. Luft, A. Szczesna, T.E. Ciuleanu, M. Dediu, R. Ramlau, R.K. Galiulin, B. Balint, G. Losonczy, A. Kazarnowicz, K. Park, C. Schumann, M. Reck, H. Depenbrock, S. Nanda, A. Kruljac-Letunic, R. Kurek, L. Paz-Ares, M.A. Socinski, S. Investigators, Necitumumab plus gemcitabine and cisplatin versus gemcitabine and cisplatin alone as first-line therapy in patients with stage IV squamous non-small-cell lung cancer (SQUIRE): an open-label, randomised, controlled phase 3 trial, Lancet Oncol. 16 (2015) 763–774.

[4] J. Rotow, T.G. Bivona, Understanding and targeting resistance mechanisms in NSCLC, Nat. Rev. Cancer 17 (2017) 637–658.

[5] I.A. Prior, P.D. Lewis, C. Mattos, A comprehensive survey of Ras mutations in cancer, Cancer Res. 72 (2012) 2457–2467.

[6] C.R. Lindsay, M. Jamal-Hanjani, M. Forster, F. Blackhall, KRAS: reasons for optimism in lung cancer, Eur. J. Cancer 99 (2018) 20–27.

[7] M. Roman, I. Baraibar, I. Lopez, E. Nadal, C. Rolfo, S. Vicent, I. Gil-Bazo, KRAS oncogene in non-small cell lung cancer: clinical perspectives on the treatment of an old target, Mol. Cancer 17 (2018) 33.

[8] C.R. Chong, P.A. Janne, The quest to overcome resistance to EGFR-targeted therapies in cancer, Nat. Med. 19 (2013) 1389–1400.

[9] B. Zhou, C. Tang, J. Li, k-RAS mutation and resistance to epidermal growth factor receptor-tyrosine kinase inhibitor treatment in patients with nonsmall cell lung cancer, J. Cancer Res. Ther. 13 (2017) 699–701.

[10] L. Seguin, S. Kato, A. Franovic, M.F. Camargo, J. Lesperance, K.C. Elliott, M. Yebra, A. Mielgo, A.M. Lowy, H. Husain, T. Cascone, L. Diao, J. Wang, I.I. Wistuba, J.V. Heymach, S.M. Lippman, J.S. Desgrosellier, S. Anand, S.M. Weis, D.A. Cheresh, An integrin beta(3)-KRAS-RalB complex drives tumour stemness and resistance to EGFR inhibition, Nat. Cell Biol. 16 (2014) 457–468.

[11] S.M. Shin, D.K. Choi, K. Jung, J. Bae, J.S. Kim, S.W. Park, K.H. Song, Y.S. Kim, Antibody targeting intracellular oncogenic Ras mutants exerts anti-tumour effects after systemic administration, Nat. Commun. 8 (2017) 15090.

[12] M.B. Ryan, R.B. Corcoran, Therapeutic strategies to target RAS-mutant cancers, Nat. Rev. Clin. Oncol. 15 (2018) 709–720.

[13] K.S. Park, H. Yang, J. Choi, S. Seo, D. Kim, C.H. Lee, H. Jeon, S.W. Kim, D.H. Lee,

The HSP90 inhibitor, NVP-AUY922, attenuates intrinsic PI3K inhibitor resistance in KRAS-mutant non-small cell lung cancer, Cancer Lett. 406 (2017) 47–53.

[14] P.A. Janne, M.M. van den Heuvel, F. Barlesi, M. Cobo, J. Mazieres, L. Crino, S. Orlov, F. Blackhall, J. Wolf, P. Garrido, A. Poltoratskiy, G. Mariani, D. Ghiorghiu, E. Kilgour, P. Smith, A. Kohlmann, D.J. Carlile, D. Lawrence, K. Bowen, J. Vansteenkiste, Selumetinib plus docetaxel compared with docetaxel alone and progression-free survival in patients with KRAS-mutant advanced non-small cell lung cancer: the SELECT-1 randomized clinical trial, J. Am. Med. Assoc. 317 (2017) 1844–1853.

[15] Y.J. Kim, K. Jung, D.S. Baek, S.S. Hong, Y.S. Kim, Co-targeting of EGF receptor and neuropilin-1 overcomes cetuximab resistance in pancreatic ductal adenocarcinoma with integrin beta1-driven Src-Akt bypass signaling, Oncogene 36 (2017) 2543–2552.

[16] Y.J. Kim, J. Bae, T.H. Shin, S.H. Kang, M. Jeong, Y. Han, J.H. Park, S.K. Kim, Y.S. Kim, Immunoglobulin Fc-fused, neuropilin-1-specific peptide shows efficient tumor tissue penetration and inhibits tumor growth via anti-angiogenesis, J. Control. Release 216 (2015) 56–68.

[17] H.F. Guo, C.W. Vander Kooi, Neuropilin functions as an essential cell surface receptor, J. Biol. Chem. 290 (2015) 29120–29126.

[18] G.J. Prud'homme, Y. Glinka, Neuropilins are multifunctional coreceptors involved in tumor initiation, growth, metastasis and immunity, Oncotarget 3 (2012) 921–939.

[19] J.C. Dong, H. Gao, S.Y. Zuo, H.Q. Zhang, G. Zhao, S.L. Sun, H.L. Han, L.L. Jin, L.H. Shao, W. Wei, S.Z. Jin, Neuropilin 1 expression correlates with the Radio-resistance of human non-small-cell lung cancer cells, J. Cell Mol. Med. 19 (2015) 2286–2295.

[20] T.M. Hong, Y.L. Chen, Y.Y. Wu, A. Yuan, Y.C. Chao, Y.C. Chung, M.H. Wu, S.C. Yang, S.H. Pan, J.Y. Shih, W.K. Chan, P.C. Yang, Targeting neuropilin 1 as an antitumor strategy in lung cancer, Clin. Cancer Res. 13 (2007) 4759–4768.

[21] S. Sun, S. Liu, S.Z. Duan, L. Zhang, H. Zhou, Y. Hu, X. Zhou, C. Shi, R. Zhou, Z. Zhang, Targeting the c-Met/FZD8 signaling axis eliminates patient-derived cancer stem-like cells in head and neck squamous carcinomas, Cancer Res. 74 (2014) 7546–7559.

[22] M.R. Yun, H.M. Choi, H.N. Kang, Y. Lee, H.S. Joo, D.H. Kim, H.R. Kim, M.H. Hong, S.O. Yoon, B.C. Cho, ERK-dependent IL-6 autocrine signaling mediates adaptive resistance to pan-PI3K inhibitor BKM120 in head and neck squamous cell carcinoma, Oncogene 37 (2018) 377–388.

[23] W. Yang, J. Soares, P. Greninger, E.J. Edelman, H. Lightfoot, S. Forbes, N. Bindal, D. Beare, J.A. Smith, I.R. Thompson, S. Ramaswamy, P.A. Futreal, D.A. Haber, M.R. Stratton, C. Benes, U. McDermott, M.J. Garnett, Genomics of Drug Sensitivity in Cancer (GDSC): a resource for therapeutic biomarker discovery in cancer cells, Nucleic Acids Res. 41 (2013) D955–D961.

[24] M. Takeda, K. Nakagawa, Role of EGFR monoclonal antibodies in the management of non-small cell lung cancer, Curr. Cancer Drug Targets 15 (2015) 792–802.

[25] L. Mazzarella, A. Guida, G. Curigliano, Cetuximab for treating non-small cell lung cancer, Expert Opin. Biol. Ther. 18 (2018) 483–493.

[26] H.P. Moll, K. Pranz, M. Musteanu, B. Grabner, N. Hruschka, J. Mohrherr, P. Aigner, P. Stiedl, L. Brcic, V. Laszlo, D. Schramek, R. Moriggl, R. Eferl, J. Moldvay, K. Dezso, P.P. Lopez-Casas, D. Stoiber, M. Hidalgo, J. Penninger, M. Sibilia, B. Gyorffy, M. Barbacid, B. Dome, H. Popper, E. Casanova, Afatinib restrains K-RAS-driven lung tumorigenesis, Sci. Transl. Med. 10 (2018) eaao2301.

[27] Q. Liu, S. Yu, W. Zhao, S. Qin, Q. Chu, K. Wu, EGFR-TKIs resistance via EGFR-independent signaling pathways, Mol. Cancer 17 (2018) 53.

[28] E. Manchado, S. Weissmueller, J.P.t. Morris, C.C. Chen, R. Wullenkord, A. Lujambio, E. de Stanchina, J.T. Poirier, J.F. Gainor, R.B. Corcoran, J.A. Engelman, C.M. Rudin, N. Rosen, S.W. Lowe, A combinatorial strategy for treating KRAS-mutant lung cancer, Nature 534 (2016) 647–651.

[29] S.D. Robinson, L.E. Reynolds, V. Kostourou, A.R. Reynolds, R.G. da Silva, B. Tavora, M. Baker, J.F. Marshall, K.M. Hodivala-Dilke, Alphav beta3 integrin limits the contribution of neuropilin-1 to vascular endothelial growth factor-induced angiogenesis, J. Biol. Chem. 284 (2009) 33966–33981.

[30] A.M. Waters, I. Ozkan-Dagliyan, A.V. Vaseva, N. Fer, L.A. Strathern, G.A. Hobbs, B. Tessier-Cloutier, W.K. Gillette, R. Bagni, G.R. Whiteley, J.L. Hartley, F. McCormick, A.D. Cox, P.J. Houghton, D.G. Huntsman, M.R. Philips, C.J. Der, Evaluation of the selectivity and sensitivity of isoform- and mutation-specific RAS antibodies, Sci. Signal. 10 (2017) eaao3332.

[31] S. Rizzolio, N. Rabinowicz, E. Rainero, L. Lanzetti, G. Serini, J. Norman, G. Neufeld, L. Tamagnone, Neuropilin-1-dependent regulation of EGF-receptor signaling, Cancer Res. 72 (2012) 5801–5811.

[32] H. Hamidi, J. Ivaska, Every step of the way: integrins in cancer progression and metastasis, Nat. Rev. Cancer 18 (2018) 533–548.

[33] L. Guo, F. Zhang, Y. Cai, T. Liu, Expression profiling of integrins in lung cancer cells, Pathol. Res. Pract. 205 (2009) 847–853.

[34] J.S. Desgrosellier, L.A. Barnes, D.J. Shields, M. Huang, S.K. Lau, N. Prevost, D. Tarin, S.J. Shattil, D.A. Cheresh, An integrin alpha(v)beta(3)-c-Src oncogenic unit promotes anchorage-independence and tumor progression, Nat. Med. 15 (2009) 1163–1169.

[35] S. Misale, J.P. Fatherree, E. Cortez, C. Li, S. Bilton, D. Timonina, D.T. Myers, D. Lee, M. Gomez-Caraballo, M. Greenberg, V. Nangia, P. Greninger, R.K. Egan, J. McClanaghan, G.T. Stein, E. Murchie, P.P. Zarrinkar, M.R. Janes, L.S. Li, Y. Liu, A.N. Hata, C.H. Benes, KRAS G12C NSCLC models are sensitive to direct targeting of KRAS in combination with PI3K inhibition, Clin. Cancer Res. 25 (2019) 796–807.

[36] A. Naik, A. Al-Yahyaee, N. Abdullah, J.E. Sam, N. Al-Zeheimi, M.W. Yaish, S.A. Adham, Neuropilin-1 promotes the oncogenic Tenascin-C/integrin beta3 pathway and modulates chemoresistance in breast cancer cells, BMC Canc. 18 (2018) 533.

[37] D. Grun, G. Adhikary, R.L. Eckert, NRP-1 interacts with GIPC1 and alpha6/beta4-integrins to increase YAP1/Np63alpha-dependent epidermal cancer stem cell survival, Oncogene 37 (2018) 4711–4722.

[38] I.S. Okon, K.A. Coughlan, C. Zhang, C. Moriasi, Y. Ding, P. Song, W. Zhang, G. Li, M.H. Zou, Protein kinase LKB1 promotes RAB7-mediated neuropilin-1 degradation to inhibit angiogenesis, J. Clin. Investig. 124 (2014) 4590–4602.

[39] S.A. Wickstrom, R. Fassler, Regulation of membrane traffic by integrin signaling, Trends Cell Biol. 21 (2011) 266–273.